

# PARTICLE TRACKING OF A COMPLEX MICROSYSTEM IN THREE DIMENSIONS AND SIX DEGREES OF FREEDOM

Craig R. Copeland<sup>1</sup>, Craig D. McGray<sup>2</sup>, B. Robert Ilic<sup>1,3</sup>, Jon Geist<sup>2</sup>, and Samuel M. Stavis<sup>1</sup>

<sup>1</sup>Microsystems and Nanotechnology Division,

<sup>2</sup>Quantum Measurement Division,

<sup>3</sup>CNST NanoFab, National Institute of Standards and Technology, Maryland USA

## ABSTRACT

We make use of the intrinsic aberrations of an optical microscope to track single particles in three dimensions, and we combine information from multiple particles on a rigid body of a microelectromechanical system to measure its motion in six degrees of freedom. Our tracking method provides an extraordinary amount of information from an ordinary imaging system, revealing unintentional motion of the microsystem due to fabrication tolerance and nanoscale clearance between parts in sliding contact. Our work facilitates quantification and study of the actuation performance and reliability of complex microsystems.

## KEYWORDS

3D, 6DOF, MEMS, metrology, microscopy, motion

## INTRODUCTION

Mechanical systems are fundamentally important to many modern technologies and have great potential for future development. Complex mechanical systems often use rigid-link mechanisms to transduce an input into an output of forces and motion to reliably perform useful work. Such transduction can involve the transfer of motion, with multiple degrees of freedom, through parts of the system in sliding contact. However, practical limitations of transduction result in an imperfect output of forces and motion, limiting performance and reliability. In particular, coupling interactions between parts in sliding contact such as play, feedback, friction, and wear can affect the system kinematics. Play and feedback can not only reduce the precision of the intentional motion of the system but can also result in unintentional and unpredictable motion of microsystems [1]. Moreover, friction and wear can become problematic at the microscale and nanoscale, due to high surface to volume ratios and lack of lubricating liquid films, motivating efforts to elucidate and mitigate these effects [2-5]. In the case that coupling interactions result in nondeterministic motion at small scales, it is necessary to measure single motion with cycles of the system to understand the true kinematics. In any case, single motion cycles are essential in a variety of applications in which the motion of the system is fundamentally aperiodic, such as positioning, switching, and gripping. However, methods to measure the single motion cycles of mechanical systems – often occurring at length scales much smaller than the parts of the system, ranging from the millimeter scale down to the atomic scale, and occurring in six degrees of freedom – have lagged behind microsystem technologies.

Methods for measuring micromechanical motion are often optical due to compatibility with the operation of the systems. Imaging methods can resolve single cycles of in-plane motion at the nanometer scale but have limits of the

magnitude or mode of motion that is measurable [6, 7], specific requirements for system design [8], or the need to fabricate test structures for imaging [9]. Interferometry methods for measuring out-of-plane motion can be precise but have only recently measured in-plane motion [10] and require scanning, impeding characterization of systems with multiple moving parts. These various limitations leave a measurement gap, presenting both opportunities and challenges for the development of complex microsystems.

To bridge this gap, we advance our method of particle tracking [1, 11-14] to provide a new capability to measure microsystem motion. We exploit the intrinsic aberrations of an optical microscope to track single particles in three dimensions on a complex microsystem [15, 16], which moves through a deep and ultrawide field. We introduce an algorithm for position estimation in three dimensions, using light-weighting [17] to robustly fit Gaussian models to images and precisely estimate image shape throughout the focal volume. Linear combinations of Zernike polynomials extend this localization analysis to a widefield calibration. A rigid transform combines information from multiple particles to measure the output motion of the microsystem in six degrees of freedom, enabling tracking of the system as it rotates through a repetitive orbit with nanoscale deviations from coupling interactions. Our new method is broadly applicable, and our measurement results provide new insight into the actuation performance and reliability of complex microsystems.

## RESULTS AND DISCUSSION

### Materials and methods

Our microscope system has an objective lens with a nominal magnification of 50 $\times$  and a numerical aperture of 0.55. A piezoelectric actuator translates the lens in the z direction with a resolution of 10 nm, providing reference values of z that we assume are accurate. A light-emitting diode illuminates the sample at a peak wavelength of approximately 625 nm. A complementary metal-oxide-semiconductor camera operating with a global shutter records fluorescence micrographs at a peak wavelength of approximately 645 nm. We calibrate the mean value of image pixel size as 127.34 nm  $\pm$  0.03 nm [17]. We report all uncertainties in this study as standard deviations, or we note otherwise. We will present further details and calibration of our microscope system in a future study.

Our test microsystem features a rotational electrostatic actuator coupling through a ratchet mechanism to a ring gear, forming a drive motor that operates in an open loop [15, 16]. The ring gear has 200 teeth that couple to a load gear with 80 teeth and a nominal diameter of 328  $\mu$ m, as Figure 1a shows. A constellation of fluorescent particles with nominal diameters of 1  $\mu$ m rides on the load gear, as Figure 1b-c shows. A square wave voltage with an

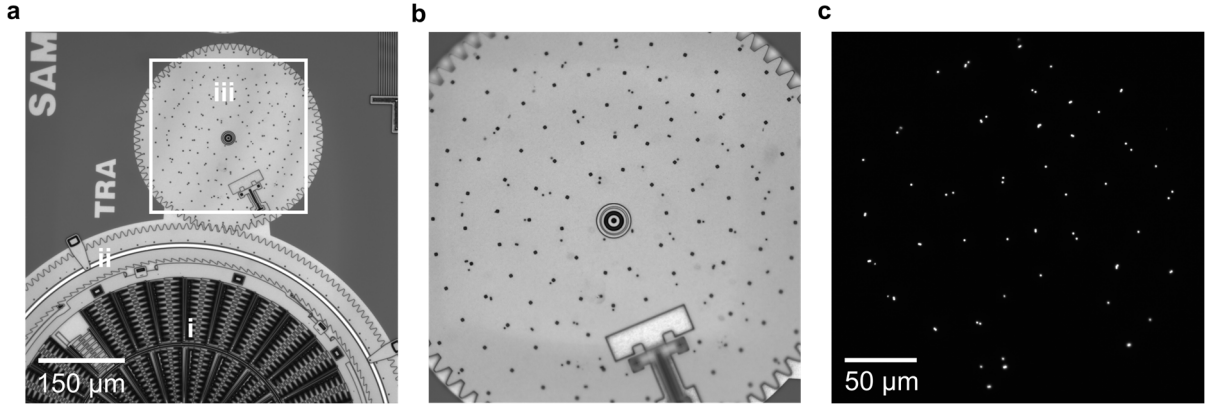


Figure 1. Experimental overview. (a) Brightfield micrograph at inspection magnification showing the drive motor, with (i) a rotational actuator, (ii) a ring gear, and (iii) the load gear. (b) Brightfield micrograph at experimental magnification showing the load gear. The smaller dots with random spacing are fluorescent particles and the larger dots in a radial pattern are etch holes for sacrificial release of the structures. (c) Fluorescence micrograph at experimental magnification showing a constellation of fluorescent particles on the surface of the load gear.

amplitude and offset of approximately 7.5 V and a frequency of approximately 90 Hz actuates the motor. Each period incrementally rotates the load gear, which we define as a single motion cycle. After each motion cycle, the microscope system records a fluorescence micrograph of the particles on the quasi-static gear, as Figure 1c shows.

We fit models to data by the method of damped least-squares with uniform weighting, or we note otherwise.

### Particle tracking in three dimensions

Intrinsic aberrations of our optical microscope affect the peak amplitudes and shapes of particle images, as Figure 2a shows, enabling localization in three spatial dimensions. We fit a bivariate Gaussian model to the image data by the light-weighting algorithm [17], exploiting the information content of multiple parameters,

$$G_{biv}(x_p, y_p) = A \cdot \exp\left(\frac{-1}{2(1-\rho^2)}\left[\frac{(x_p-x)^2}{\sigma_x^2} - 2\rho\frac{(x_p-x)(y_p-y)}{\sigma_x\sigma_y} + \frac{(y_p-y)^2}{\sigma_y^2}\right]\right) + B$$

where  $(x_p, y_p)$  is the position of a pixel in a micrograph,  $(x, y)$  is the position of the Gaussian peak,  $A$  is the peak

amplitude,  $\sigma_x$  is the standard deviation in the x direction,  $\sigma_y$  is the standard deviation in the y direction,  $\rho$  is the correlation coefficient between the x and y directions, and  $B$  is a constant background. Division of  $\rho$  by the amplitude parameter  $A$ ,  $\rho_{amp} = \rho/A_n$ , where  $A_n = A/A_{\rho=\rho^*}$  is the amplitude parameter after normalization to its value in the particular image for which  $\rho = \rho^*$ , provides a useful z dependence, as Figure 2b shows. This normalization ensures that any differences in fluorescence intensity between the particles for calibration and for experiment do not affect the calibration of z dependence. We set  $\rho^*$  to the minimum value of  $|\rho|$ . The statistical uncertainty of axial localization from empirical polynomial models of  $z(\rho_{amp})$ , such as Figure 2b shows, is approximately 50 nm and is due primarily to the random noise in  $\rho_{amp}$ . To accurately calibrate the lateral dependence of the relationship in Figure 2b, we deposit a random array of calibration particles onto a silicon substrate and image the particles through focus, sampling the field to obtain a set of local calibration functions  $[z(\rho_{amp})]_{cal}$ . The z positions from this set of calibration functions vary significantly across the lateral extent of the field of 260  $\mu\text{m}$  by 260  $\mu\text{m}$ , as Figure 2c shows for a representative value of  $\rho_{amp} = -0.1$ .

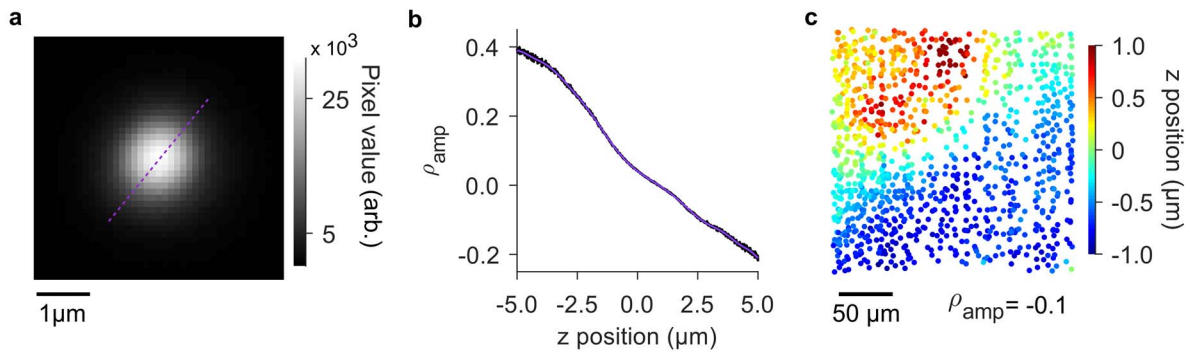


Figure 2: Axial localization. (a) Optical micrograph showing an image of a fluorescent particle with a diameter of approximately 1  $\mu\text{m}$  at a z position of 2  $\mu\text{m}$  above best focus. The dash violet line indicates the major axis. (b) Plot showing a representative dependence of the shape parameter  $\rho_{amp} = \rho/A_n$  on z position, where  $\rho$  is the correlation coefficient and  $A_n$  is the normalized amplitude of a bivariate Gaussian model. The solid violet line shows a polynomial of order 16, which empirically models the z dependence for axial localization. (c) Plot showing the lateral dependence of z position for a common value of the shape parameter  $\rho_{amp} = -0.1$  from a random array of calibration particles that sample the imaging field. Uncertainties in (c) are smaller than the data markers.

To develop our widefield calibration, we model this lateral dependence by linear combinations of Zernike polynomials. The residuals of this model fit to data such as in Figure 2c define systematic errors of axial localization, which have root-mean-square values of approximately 70 nm. These errors are due primarily to variation of image shape at lateral scales of a few micrometers, as Figure 2c shows. We perform analogous calibrations for the axial and lateral dependence of apparent lateral motion. We will elucidate these results, as well as the precision and accuracy of our method, in a future study.

### Microsystem tracking in six degrees of freedom

A rigid transform maps particle positions between subsequent micrographs by the iterative closest-point algorithm, yielding the motion of the gear for each cycle. The center of rotation is a natural origin of our extrinsic coordinate system, which we determine as the mean value of all particle positions in each dimension over multiple revolutions of the gear. The residuals of the rigid transforms confirm the accuracy of tracking single particles to within root-mean-square errors of approximately 2 nm in  $x$  and  $y$  and approximately 80 nm in  $z$ . The rigid transform determines three translations  $\Delta x$ ,  $\Delta y$ , and  $\Delta z$ , and three rotations in as many degrees of freedom, the intrinsic rotation of the gear  $\gamma$  about the axis of rotation, the nutation  $\beta$  of the axis of rotation with respect to the extrinsic  $z$  axis, and the precession  $\alpha$  of the axis of rotation about the extrinsic  $z$  axis, as Figure 3 shows. Uncertainties of these

six degrees of freedom depend on the particular particle constellation and the extrinsic coordinate system [13, 18], as we will describe in a future study.

Our measurements show significant variation in four of the six degrees of freedom due to play in the couplings between the parts of the microsystem, as Figure 3 shows. These results provide new insight into how the parts of complex microsystems move during operation, including both intentional and unintentional motion at nanometer and milliradian scales. Clearance between the meshing teeth of the ring and load gears, as well as variability of the rotational actuator [12], cause variability of the intrinsic rotation  $\gamma$  in Figure 3a. Clearance between the gear and the hub causes variability of the translations  $\Delta x$  and  $\Delta y$  that Figure 3d,e shows. Clearance between the gear and the underlying substrate allows for nutation  $\beta$  of the axis of rotation relative to the extrinsic  $z$  axis, as Figure 3c shows. The gear does not exhibit significant translation in the  $z$  direction  $\Delta z$ , as Figure 3f shows, which validates the measurement uncertainty for translations in this direction. While the precession of the axis of rotation  $\alpha$  varies over a wide range, as Figure 3c shows, the small nutation  $\beta$  that Figure 3b shows causes the rigid transform to be relatively insensitive to this degree of freedom, so that nearly all of the variability is within measurement uncertainty. A different selection of reference frame could improve some of these uncertainties while degrading others. We will analyze these results in more detail in a future study.

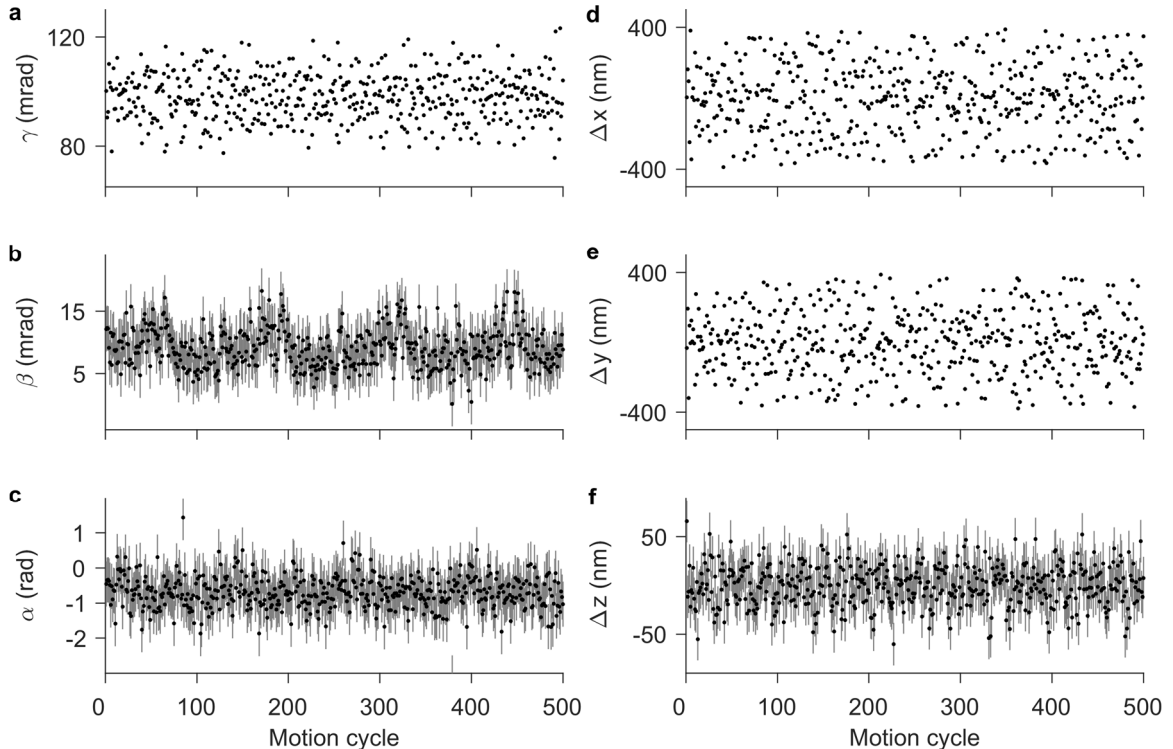


Figure 3: Microsystem tracking. (a-c) Plots showing (a) intrinsic rotations of the gear in three-dimensional space  $\gamma$ , (b) the angle between the axis of rotation and the extrinsic  $z$  axis, or nutation  $\beta$ , and (c) the angle between the axis of rotation and the extrinsic  $x$ - $z$  plane, or precession  $\alpha$ . Variability in (a-c) is due to rotational play in three dimensions. (d-f) Plots showing translation of the gear in the (d)  $x$ , (e)  $y$ , and (f)  $z$  directions. Variability in (d) and (e) indicates translational play, with effective ranges of 394 nm and 387 nm, respectively, while variability in (f) is due to measurement uncertainty. Uncertainties in (a, d, e) are smaller than data markers.

## CONCLUSIONS

We introduce a method of particle tracking in three dimensions to measure the motion of a microscale rigid body with six degrees of freedom. Rigid transforms allow the combination of localization data to improve centroid and orientation precision through the central limit theorem [13], now in three dimensions. While such analysis is common in motion tracking of macroscale objects, this is the first such application in particle tracking by optical microscopy. Our new method enables study of a complex microsystem. We find that microfabrication tolerance and nanoscale clearance between parts in sliding contact not only degrade the precision of the intentional motion of the test system, but also result in unintentional motion that is orthogonal to the primary plane of the test system and occurs in all six degrees of freedom. These results provide insight into actuation performance and reliability. While our test system dates back two decades and is commercially available, its ultraplanar fabrication process remains near the state of the art, and we are unaware of any previous measurement that reveals the complex kinematics resulting from nanoscale clearances within such a system. Moreover, commercial microsystems still do not make full use of the complexity that such processes enable, and indeed most microsystems have simpler kinematics than our test system. Advancing practical methods to quantify and specify the motion of complex microsystems will help to fulfill their potential for many exciting applications.

## ACKNOWLEDGEMENTS

The authors acknowledge support under the NIST Innovations in Measurement Science program. C.R.C. acknowledges support under the Cooperative Research Agreement between the University of Maryland and the National Institute of Standards and Technology Center for Nanoscale Science and Technology, Award 70NANB10H193, through the University of Maryland.

## REFERENCES

- [1] C. R. Copeland, C. D. McGray, J. Geist, V. A. Aksyuk, and S. M. Stavis, "Transfer of motion through a microelectromechanical linkage at nanometer and microradian scales," *Microsystems & Nanoengineering*, Article vol. 2, 2016.
- [2] I. Rosenhek-Goldian, N. Kampf, A. Yeredor, and J. Klein, "On the question of whether lubricants fluidize in stick-slip friction," *Proceedings of the National Academy of Sciences*, vol. 112, no. 23, pp. 7117-7122, 2015.
- [3] A. Vijayasai, G. Sivakumar, G. Ramachandran, C. Anderson, R. Gale, and T. Dallas, "Characterization of a MEMS tribogauge," *Surface and Coatings Technology*, vol. 215, no. 0, pp. 306-311, 2013.
- [4] T. D. B. Jacobs and R. W. Carpick, "Nanoscale wear as a stress-assisted chemical reaction," *Nat Nano*, vol. 8, no. 2, pp. 108-112, 2013.
- [5] F. W. DelRio, M. P. de Boer, J. A. Knapp, E. David Reedy, P. J. Clews, and M. L. Dunn, "The role of van der Waals forces in adhesion of micromachined surfaces," *Nature Materials*, vol. 4, no. 8, pp. 629-634, 2005.

- [6] D. M. Freeman, "Measuring Motions of MEMS," *MRS Bulletin*, vol. 26, no. 04, pp. 305-306, 2001.
- [7] *MSA 500 Hardware Manual*. Polytec (Hopkinton, MA).
- [8] C. Yamahata, E. Sarajlic, G. J. M. Krijnen, and M. A. M. Gijs, "Subnanometer Translation of Microelectromechanical Systems Measured by Discrete Fourier Analysis of CCD Images," *J. Microelectromech. Syst.*, vol. 19, no. 5, pp. 1273-1275, 2010.
- [9] P. Cheng and C. H. Menq, "Real-Time Continuous Image Registration Enabling Ultraprecise 2-D Motion Tracking," (in English), *IEEE Trans. Image Process.*, Article vol. 22, no. 5, pp. 2081-2090, 2013.
- [10] C. Rembe, R. Kowarsch, W. Ochs, A. Dräbenstedt, M. Giesen, and M. Winter, "Optical three-dimensional vibrometer microscope with picometer-resolution in x, y, and z," *OPTICE*, vol. 53, no. 3, pp. 034108-034108, 2014.
- [11] C. R. Copeland, C. D. McGray, J. Geist, V. A. Aksyuk, and S. M. Stavis, "Characterization of electrothermal actuation with nanometer and microradian precision," in *Solid-State Sensors, Actuators and Microsystems (TRANSDUCERS), 2015 18th International Conference on*, 2015, pp. 792-795.
- [12] C. R. Copeland, C. D. McGray, J. Geist, and S. M. Stavis, "Particle tracking of microelectromechanical system performance and reliability," *J. Microelectromech. Syst.*, vol. 27, no. 6, pp. 948-950, 2018.
- [13] C. McGray, C. R. Copeland, S. M. Stavis, and J. Geist, "Centroid precision and orientation precision of planar localization microscopy," *Journal of Microscopy*, pp. 238-249, 2016.
- [14] C. D. McGray *et al.*, "MEMS Kinematics by Super-Resolution Fluorescence Microscopy," *J. Microelectromech. Syst.*, vol. 22, no. 1, pp. 115-123, 2013.
- [15] S. M. Barnes, S. L. Miller, M. S. Rodgers, and F. Bitsie, "Torsional ratcheting actuating system," in *2000 International Conference on Modeling and Simulation of Microsystems, Technical Proceedings*, M. Laudon and B. Romanowicz, Eds., 2000, pp. 273-276.
- [16] D. M. Tanner *et al.*, "Reliability of a MEMS Torsional Ratcheting Actuator," in *39th Annual Proceedings: International Reliability Physics Symposium 2001*, 2001, pp. 81-90.
- [17] C. R. Copeland *et al.*, "Subnanometer localization accuracy in widefield optical microscopy," *Light: Science & Applications*, vol. 7, 2018.
- [18] M. Shah, M. Franaszek, and G. Cheok, "Propagation of Error from Registration Parameters to Transformed Data," *Journal of Research of the National Institute of Standards and Technology*, vol. 121, 2016.

## CONTACT

\*S.M. Stavis, samuel.stavis@nist.gov